NANO LETTERS

2001
Vol. 1, No. 3
129−135

Nanoparticle Arrays Formed by Spatial Compartmentalization in a Complex Fluid

Millicent A. Firestone,[†,*] Dixy E. Williams,[†,§] Sönke Seifert,[‡] and Roseann Csencsits[†]

Materials Science and Chemistry Divisions, Argonne National Laboratory, 9700 South Cass Avenue, Argonne, Illinois 60439

Received January 4, 2001

ABSTRACT

A mesoscopically ordered lamellar gel phase of a polymer-grafted, lipid-based complex fluid is used as a scaffolding to spatially organize inorganic nanoparticles. The complex fluid provides both a highly anisotropic environment and a segregated aqueous and organic domains in which inorganic nanoparticles can be selectively placed by tailoring their size and surface characteristics. Three types of silver nanoparticles—underivatized, surfactant-stabilized, and dodecanthiol-derivatized—were evaluated. Comparison of the surface plasmon resonance of the various silver particles dispersed in conventional solvents to those contained within the complex fluid was used to determine the region of spatial localization in the lamellar gel phase. Silver particles rendered hydrophobic by capping with an alkane thiol insert into the hydrocarbon bilayer region. Surfactant-stabilized and underivatized silver nanoparticles reside in the aqueous channels, with the latter particles preferentially interacting with the grafted PEG chains/charged membrane interface region. Interparticle interaction between encapsulated hydrophilic silver particles can be enhanced by increasing the number of PEG repeat units (i.e., the length of the lipid-appended polymer). Examination of the X-ray diffraction profiles indicates that the gel-phase structure of the complex fluid is preserved upon introduction of all three types of nanoparticles. Guinier analysis of the low-q SAXS data for the intercalated silver yields particle sizes that are in good agreement with those determined by TEM prior to introduction, indicating that they remain as nonaggregated, discrete nanoparticles. These results not only demonstrate the use of complex fluids as a matrix in which to produce periodic arrays of encapsulated nanoparticle guests, but also suggest the possibility of employing them to modulate interactions between guests and, hence, their optical and electronic properties.

Fabrication represents one of the most important challenges for the realization of technologically useful nanoparticle-based materials. Optimization of such materials depends not just on the quality of the nanoparticles (e.g., size and shape) and their surface chemistry, but also on their spatial orientation and arrangement. The development of practical strategies for the assembly of inorganic nanoparticles into well-defined arrays is thus an area of considerable current interest, because it offers both opportunities to exploit their unique optical and electronic properties and possibilities to probe new, potentially collective phenomena. Much effort has focused on the formation of organized 2-D and 3-D arrays of nanoparticles by modification of particle surface chemistry and application of Langmuir−Blodgett,[1] controlled solvent evaporation,[2−4] electrophoretic,[5] or nanolithographic techniques[6] on suitable substrates.[7] More recently, biologically programmed (recognition driven) assembly, such as the use of complementary DNA oligonucleotides[8,9] or protein recognition chemistry (e.g., streptadvidin−biotin),[10,11] has also been successfully employed. However, these approaches suffer from several drawbacks that limit full exploitation of these materials, among them, the ability to generate only relatively simple structures or to organize only one type of nanoparticle and the lack of structural tailorability. An alternative strategy involves layer-by-layer superlattice assembly by the sequential adsorption of nanoparticles and either bifunctional cross-linking molecules[12−14] or oppositely charged layers of polyelectrolytes.[15] Although these methods permit the formation of heterostructures consisting of alternating layers of, for example, semiconductors and metal particles, the formation of such assemblages is a cumbersome, multistep process in which each adsorption step must be followed by washing and drying. Furthermore, these materials typically require substrates such as glass or gold to support the formed multilayers, which may ultimately restrict their range of applications. Recognition of these drawbacks has led to an ongoing search for novel methodologies for the production of supramolecular architectures comprising ordered arrays of inorganic nanoparticles. To

* To whom correspondence should be addressed. Phone: 630-252-8298. Fax: 630-252-9151. E-mail: firestone@anl.gov.
† Materials Science Division, Argonne National Laboratory.
‡ Chemistry Division, Argonne National Laboratory.
§ D.E.W. was a DOE-ANL undergraduate research participant from Oklahoma Baptist University, Shawenee, OK 74804.

10.1021/nl0155025 CCC: $20.00
Published on Web 02/28/2001

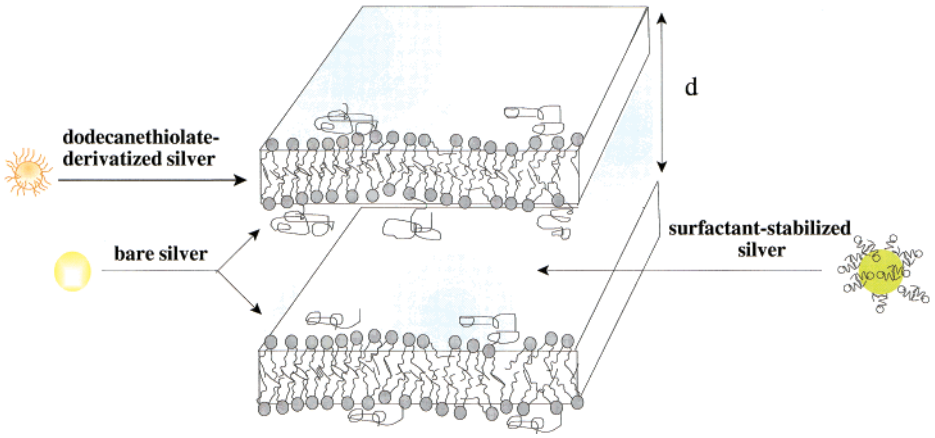

Figure 1. Schematic representation of polymer-grafted lipid-based liquid crystalline gel phase with lamellar repeat distance, *d*, used as the encapsulating matrix for the localization of Ag nanoparticles. This representation depicts the three physicochemically distinct regions of the systems and the type of nanoparticle which can be spatially directed into it: (I) surfactant-stabilized colloidal Ag into bulk water channels, (II) underivatized colloidal Ag into the charged-membrane-polymer (i.e., palisade) region, and (III) dodecanethiol-derivatized Ag nanoparticles into the alkane bilayer.

date, relatively little effort has been directed at an examination of the use of mesoscopically ordered soft matter as a medium in which to organize nanoparticles.[16,17] Such an approach may offer advantages in simplicity of construction, enhanced processability, and the facile generation of heterostructured materials.

In this work, we demonstrate that complex fluids can serve as a scaffolding for the spatial localization of inorganic nanoparticles. Specifically, silver nanoparticles are organized into a processable (e.g., by externally applied magnetic fields), polymer-grafted, lipid-based complex fluid consisting of a quaternary mixture of water, a phospholipid (dimyristoylphosphatidylcholine), a polymer comprising poly(ethylene) glycol (PEG) terminally grafted onto the headgroup of a phospholipid (dimyristoylphosphatidylethanolamine), and a zwitterionic surfactant (*N*,*N*-dimethyldodecylamine *N*-oxide). In a previous report, we described the preparation of this complex fluid and its structural characterization by a variety of spectroscopic and scattering techniques.[18] Briefly, at room temperature, the amphipathic components spontaneously organize in water to form an elastic solid (gel) consisting of ordered microdomains of lamellae (Figure 1), whereas below the phase transition (16 °C), the material exists in a lower viscosity state as a 2-D hexagonal array of prolate micelles. Small-angle neutron scattering studies of the lamellar gel phase structure of the complex fluid have shown it to consist of alternating organic sheets (alkane bilayers) ca. 35 Å thick and aqueous channels 105−135 Å in thickness. Our subsequent work has demonstrated that exploitation of the inverted, thermoreversible phase transition in the presence of an applied magnetic field provides a facile means of aligning the lamellar microdomains, thereby eliminating unfavorable orientation and defects in this material and extending the order into macroscopic dimensions.[19] In the present work, we examine how this phase, which features three physicochemically distinct regions (i.e., a hydrocarbon bilayer region, a charged membrane-polymer interfacial region, and bulk water channels) can be used to incorporate and spatially compartmentalize inorganic nanoparticles (Figure 1). In particular, we demonstrate that by controlling their surface chemistry and size, silver nanoparticles can be selectively positioned in defined regions of the encapsulating matrix. Furthermore, we present preliminary data suggesting that interactions between particles can be "tuned" by adjustment of the matrix composition.

Three types of silver nanoparticles were employed in this work: bare (i.e., underivatized), surfactant-stabilized, and dodecanthiol-derivatized particles. Underivatized nanoparticles were prepared using a standard hydrosol synthesis procedure that involves the reduction of Ag(I) ions with $NaBH_4$ in aqueous solution.[20] This procedure yielded a transparent, yellow solution containing spherical particles ranging from 60 to 80 Å in diameter (mean particle diameter of 72 Å), as evidenced by transmission electron microscopy.[21] Surfactant-stabilized silver nanoparticles, which are of interest because of their enhanced stability in solution and resistance to particle aggregation,[22] were prepared by reduction of silver ions in the presence of lithium dodecyl sulfate ($C_{12}H_{25}SO_4Li$, LDS). Like the underivatized silver, the LDS-stabilized nanoparticles yielded a bright yellow solution in water.[20] However the latter particles were of higher polydispersity (60−100 Å) and had a slightly greater mean particle diameter (87 Å). Hydrophobic (dodecanethiol-derivatized) silver nanoparticles were prepared by extraction of aqueous silver ions into an organic phase with the aid of a phase transfer agent, followed by reduction with sodium borohydride in the presence of dodecanethiol ($C_{12}H_{25}SH$).[23,24] The orange-brown solid dodecanthiol-derivatized silver isolated from this procedure comprised a more monodisperse collection of spherical particles, with diameters ranging from 30 to 45 Å. Comparison of the dimensions of the segregated domains within the lamellar gel phase, Lαg, (vide supra) to those of the various silver nanoparticles indicates that both the bare silver, and the LDS-derivatized nanoparticles could be readily accommodated in the aqueous domains. Similarly, the dodecanthiol-derivatized nanoparticles are of a size commensurate with the hydrophobic alkane bilayer region.

Absorption spectroscopy was used to assess the influence of confinement in the complex fluid on the properties of the nanoparticles. In general, metal nanoparticles exhibit intense optical bands in the visible region arising from excitation of localized surface plasmon resonances (collective oscillations of conduction electrons). The wavelength corresponding to the extinction maximum, as well as the shape and amplitude of the bands, are indicative of their particle size, state of aggregation, and chemical environment. The plasmon absorption band of silver nanoparticles has been shown to be particularly sensitive to particle-adsorbate interactions (e.g., changes in the dielectric properties of the metal particles induced by chemi- or physisorption) and to changes in the immediate chemical environment of the particles arising from, for example, alterations in the refractive index of the surrounding medium.[25,26] The UV−vis absorption spectrum of freshly prepared bare silver particles in aqueous solution (hydrosol) was compared to that obtained for the same particles incorporated within the Lαg phase of a complex fluid based on a phospholipid appended with poly(ethylene)-glycol having 45 monomer units, PEG2000 (Figure 2A, plots a and b, respectively).[27] As shown, both spectra feature the narrow, symmetric surface plasmon resonances characteristic of nonaggregated, spherical silver particles (centered at 395 and 402 nm, respectively). Unlike other metal nanoparticles, for colloidal silver, it has been established that the position of the plasmon resonance is relatively insensitive to alterations in particle size.[28] Rather, red shifts in its absorption band, as well as broadening of the resonance, have been previously shown to arise from anion association or interaction with nucleophiles (which may act to donate electron density into the particles).[25,26] Thus, the slight (7 nm) red shift in the position of the resonance for the nanoparticles encapsulated within the Lαg phase is undoubtedly a reflection of a change in their chemical environment relative to those dispersed in water (colloidal solution), perhaps, preferential association of the silver particles with the grafted PEG chains in the palisade layer of the complex fluid, leading to electron donation to the silver particles by the oxygen atoms of the PEG chains. Furthermore, the close correspondence of the two spectra, in particular the absence of an increased absorption tail (wing) at longer wavelengths suggests that the nanoparticles remain as individual particles rather than forming aggregates upon spatial confinement within the complex fluid.[17]

The UV−vis spectrum of surfactant-stabilized silver particles in water (Figure 2B, plot a) exhibits a peak centered at 406 nm.[29] The slight red shift of the surface plasmon resonance observed for the LDS-stabilized hydrosol relative to the bare silver hydrosol is believed it arise from the loosely associated LDS bilayer shell surrounding the nanoparticles, which consists of a first layer of LDS molecules with the hydrophilic $-SO_4^-$ moieties oriented inward and their hydrophobic $-C_{12}H_{25}$ chains pointing outward, and a second layer with the opposite orientation.[22] Unlike the underivatized nanoparticles, the introduction of these particles into the gel results in no apparent change in the position of the absorption maximum (Figure 2B, plot b), indicating that no significant

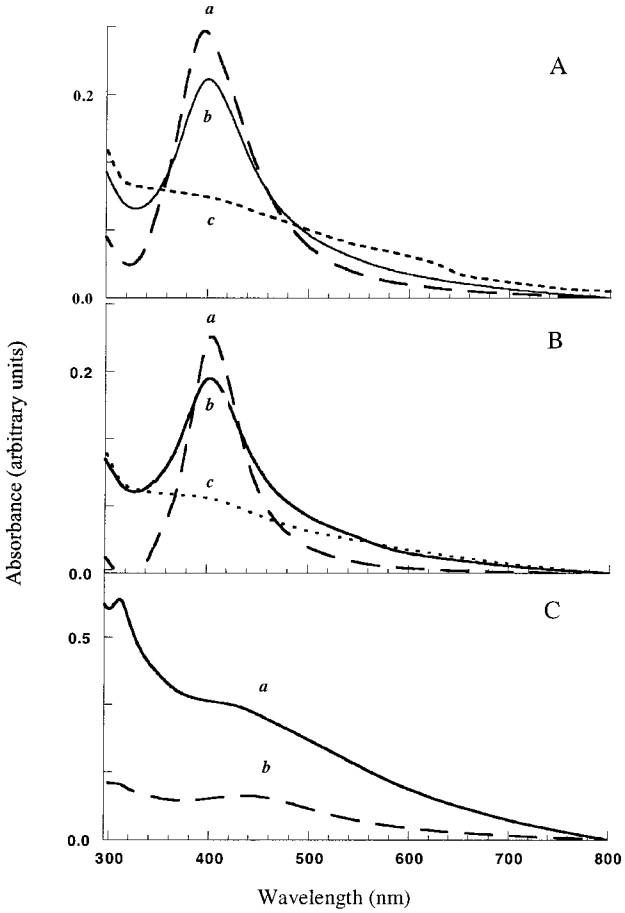

Figure 2. UV-vis absorption spectra collected on (A) 1×10^{-4} M underivatized Ag nanoparticles in (a) aqueous solution, (b) doped into PEG2000-grafted lipid compositions of the complex fluid, and (c) doped into PEG5000-grafted lipid compositions of the complex fluid; (B) 1×10^{-4} M lithium dodecyl sulfate (LDS)-stabilized Ag nanoparticles in (a) aqueous solution, (b) doped into PEG2000-grafted lipid compositions of the complex fluid, (c) doped into PEG5000-grafted lipid compositions of the complex fluid; and (C) hydrophobic dodecanthiol-capped Ag nanoparticles in (a) PEG2000-based composition and (b) dispersed in hexane. All spectra recorded at 21 °C using a Shimadzu 1601 spectrophotometer at a spectral resolution of 2 nm.

change in the chemical environment of the doped nanoparticles occurs and, thus, that these particles reside preferentially in the bulk water channels. Collectively, these results (in particular, the red shift of the surface plasmon resonance upon stabilization of the nanoparticles with a shell of LDS in water and their apparent preference to remain in the bulk water channels upon intercalation into the complex fluid) provide support for the hypothesis that the bare silver nanoparticles are associated with the grafted PEG chains upon inclusion into the complex fluid. However, determination of the exact nature of the interaction of the bare silver nanoparticles with the palisade region awaits further experimentation.

The possibility of organizing silver nanoparticles among the alkyl chains of the membrane bilayer of the Lαg phase (Figure 1) was evaluated by rendering their surface hydrophobic (i.e., derivatizing the particles with a C_{12}-alkane) and comparing the UV−vis absorption spectrum of the hydro-

phobic, dodecanthiol-derivatized silver particles in hexane to that observed for the same particles dispersed as a dry powder into the Lαg phase of the complex fluid (Figure 2C). Both spectra display a broad, metal plasmon resonance band in the visible region centered at 436 nm and a minor feature at 311 nm. The position of the metal plasmon band (i.e., that is, significantly red-shifted relative to that of the hydrosol silver nanoparticles) is consistent with alkane-derivatized silver nanoparticles and has been attributed to changes in the particle surface/interface induced by the formation of a thick dielectric coating around the particles.[30,31] The reduction in band intensity (i.e., the damping of the plasmon band in organosols relative to the hydrosols) is not fully understood, but is believed to arise from changes in the electronics of the surface layer.[32] The good correspondence between spectra in hexane solution and in the complex fluid indicates that dodecanethiol-derivatized silver nanoparticles can be successfully incorporated into the complex fluid and that they likely reside in the alkane-rich lipid bilayer region. Taken together, the results of hydrosol and organosol doping of the Lαg phase demonstrate the possibility of exploiting the interactions of appropriately derivatized nanoparticles with the various regions of a complex fluid as a means of directing their site of localization within the various physicochemical environments afforded by structured media.

To determine the effect of changes in complex fluid composition on the extent of interaction and, thus, the optical and electronic properties of spatially confined silver nanoparticles, the number of repeat units (i.e., the chain length) of the lipid-grafted poly(ethylene) glycol chains was doubled (113 PEG repeat units, PEG5000)[27] and the effect on the absorption spectra of encapsulated hydrophilic (underivatized or LDS-stabilized) silver nanoparticles examined (Figures 2A, plot c and 2B, plot c, respectively). In both instances, only broad, nearly featureless absorbance bands centered at ca. 408 and 406 nm, respectively, are observed, and significant damping of the plasmon oscillation occurs, despite the presence of a concentration of silver colloid equal to that introduced into the complex fluid based on PEG2000. The position of the peak maximum for the surfactant-coated silver nanoparticles is unchanged relative to its position in aqueous solution or in the PEG2000 based complex fluid, however. In contrast, a slight further red shift is observed for the bare silver, again suggesting association of the nanoparticles with the grafted PEG chains. This type of absorbance "signature" (broadening and decreased band amplitude) has previously been attributed to either strongly interacting silver particles or agglomerates.[17,33] Interestingly, however, none of the samples exhibits any evidence of the black precipitate that would accompany the growth of particles and their exclusion/separation from the complex fluid. Thus, the observed changes in the absorbance bands upon increasing the PEG chain length from 45 to 113 repeat units are likely the consequence of enhanced particle−particle interactions arising from spatial confinement and/or compression of the dimensions of the water channel by the tethered polymer, which may facilitate the lateral organization of the silver particles. These results are in contrast to those reported for the doping of silver nanoparticles into a lamellar phase of the water/SDS/hexanol/dodecane system, for which it has been found that as the dimensions of the water channel are reduced (in this case, by lowering the water content), agglomeration and eventual exclusion of the nanoparticles from the phase occurs.[17]

The response of the lamellar gel phase of the complex fluid to the introduction of hydrophilic silver nanoparticles (both underivatized and LDS surfactant-stabilized) was assessed by small-angle X-ray scattering (SAXS).[34] SAXS has proven to be an ideal method for the study of hydrogels, because it is nondestructive, requires no special sample preparation, and probes sample structure on the mesoscopic length scale (nm-μm). The SAXS profile collected on an undoped, Lαg phase (PEG2000) is presented in Figure 3A. The pattern is dominated by four Bragg peaks of integral order (q = 0.045, 0.091, 0.136, and 0.180 Å^{-1}), which is indicative of a lamellar structure. The position of the first-order diffraction peak corresponds to a repeat distance, d, of 140 Å (Figure 1). Typical SAXS profiles recorded for the gel phase prepared by hydration of the organic amphiphiles with either a 1×10^{-4} M solution of freshly prepared bare silver colloid or surfactant-stabilized (LDS) silver colloid are presented in Figure 3B and C, respectively. Both diffraction profiles display the same periodic structure of a lamellar phase, as evidenced by diffraction peaks that occur at integer multiples of the first-order reflection (q = 0.045 Å^{-1}), and thus, the same periodicity of 140 Å. One noticeable difference between the profiles for the doped and undoped hydrophilic Ag is the appearance in the latter of appreciable scattered X-ray intensity in the low q region that arises from the solution scattering of silver nanocrystals. Although qualitative comparison of these scattering profiles indicates no gross structural changes (i.e., the material remains lamellar) upon incorporation of the silver hydrosols into the liquid crystalline matrix, some evidence of a loss in long-range structural ordering is apparent from an increase in the breadth the diffraction peaks, suggesting that doping leads to a reduction in spatial coherence (i.e., increased lattice disorder and orientational disorder) and, hence, more poorly aligned microdomains of lamellae.

The changes in long-range ordering can be further assessed as a function of dopant by analysis of the diffraction peaks with the Scherrer equation. This equation permits an estimation of the size of the quasi-crystalline regions/zones, L, from the fwhm of the Gaussian fitted Bragg peaks and the wavelength of incident radiation.[35] Such an analysis carried out on the second-order Bragg peaks for the undoped and the hydrophilic silver nanoparticle doped hydrogel indicates that the size of the quasi-crystalline domains decreases from 307 nm for the undoped gel to 254 and 204 nm for the bare silver colloid doped and the LDS-derivatized doped hydrogel, respectively (first order reflections were not used due to the presence of low q scattering arising from the included nanoparticles). The greater reduction in average domain size for the LDS-coated silver samples may be the result of some loss (i.e., desorption of the weak, electrostatically bound) of the LDS surfactant coating from the silver nanoparticles,

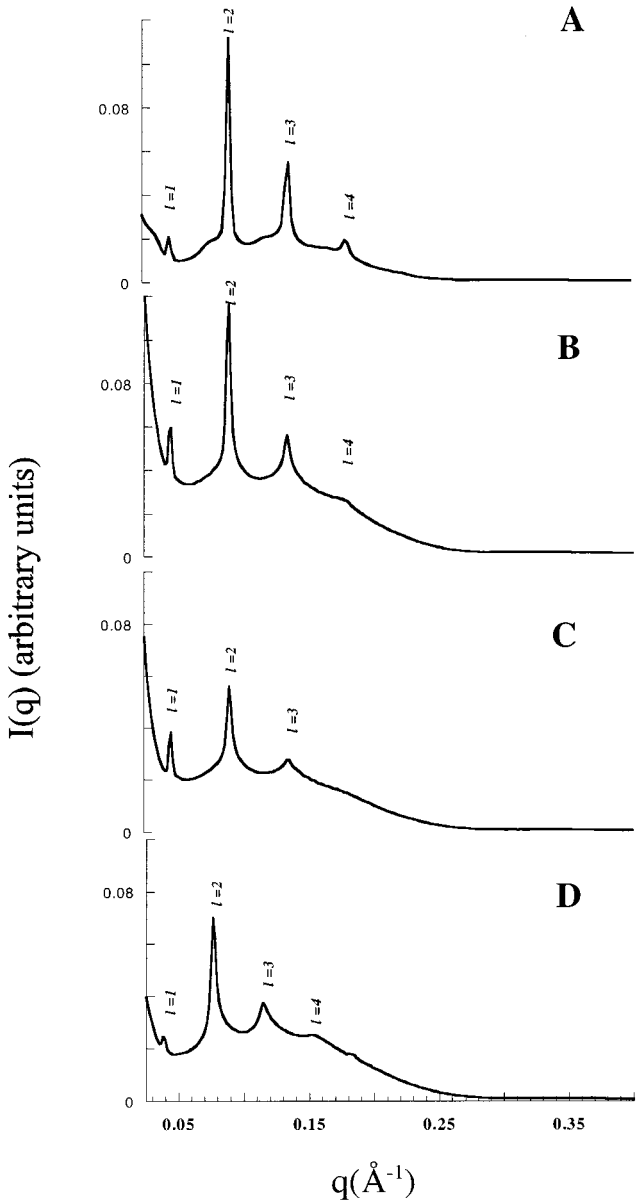

Figure 3. Synchrotron small-angle X-ray scattering profiles collected for PEG2000 grafted lipid complex fluid compositions at 23 °C (A) undoped, (B) doped with 10^{-4} M underivatized Ag silver nanoparticles (C) doped with 10^{-4} M LDS stabilized Ag silver nanoparticles (D) dodecanthiol-derivatized Ag silver nanoparticles.

which may incorporate into the complex fluid, thereby reducing the structural ordering/organization of the amphiphilic components. Despite this modest decrease in long range ordering upon nanoparticle doping, this system exhibits minimal structural perturbations upon encapsulation of hydrophilic nanoparticles. Furthermore, the loss in spatial coherence upon nanoparticle doping does not represent a major limitation in the use of these materials as a platform for nanoparticle-based composites because it has been previously shown that defects within the complex fluid can be efficiently removed by post-self-assembly magnetic field processing, yielding a macroscopically aligned (i.e., a near monodomain liquid crystal).[19] Future studies will examine in-situ synthesis of hydrophilic metal nanoparticles within the aqueous domains, since recent studies of Pt nanoparticle synthesis within polyelectrolyte hydrogels have demonstrated that under certain reaction conditions, internal structural ordering greater than that of the native gels can be achieved.[16]

Results of SAXS studies on samples incorporating the dodecanthiol-derivatized (hydrophobic) silver nanoparticles into liquid-crystalline compositions based on PEG2000-grafted lipid were similarly examined (Figure 3D). As was the case for materials doped with hydrophilic nanoparticles, the scattering profile features four diffraction peaks with a *d* spacing ratio of integral order. The position of the first-order Bragg peak ($q = 0.038$ Å^{-1}) indicates, however, that particle doping into the lipid bilayer region is accompanied by a notable increase (ca. 25 Å) in the lattice spacing (from 140 to 165 Å). This increase may arise from incorporation of nanoparticles that are of approximately the same dimensions as the hydrocarbon bilayer region and the concomitant adjustment of this region to accommodate them. Interestingly, however, insertion of these particles does not cause the formation of an unstable hybrid phase as observed for other lyotropic lamellar systems. [17] Scherer analysis for the hydrophobic Ag nanoparticle-doped material yields results consistent with those reported for the hydrophilic silver nanoparticle doped materials (L = 208 nm). Despite these changes, the overall integrity of the lamellar structure remains intact. Thus, the complex fluids are able to accommodate these nanocrystals with retention of structural integrity via adjustment of the lattice parameters.

Because dramatic alterations in the surface plasmon resonance of hydrophilic silver nanoparticles were observed upon their incorporation into the PEG5000-based composition of the complex fluid, their effect on the mesoscopic structural ordering of the liquid crystalline phase was evaluated. In general, the SAXS patterns for these compositions are characterized by a higher degree of long-range translational ordering, as evidenced by the narrower diffraction peaks, and an increase in the number of resolvable Bragg peaks (six).[19] For the undoped samples, the positions of the six peaks, which occur at integer multiples of $q = 0.037$ Å^{-1}, are indicative of a lamellar structure with a periodicity of 170 Å. Doping the samples with either the bare silver or surfactant-stabilized (LDS) silver nanoparticles does not cause any gross changes in the lamellar structure (lattice spacing 170 Å). As reported for the PEG2000 compositions, however, Scherrer analysis reveals a reduction in the size of the quasi-crystalline domains upon nanoparticle intercalation.

As noted earlier, doping of the various types of nanoparticles into the complex fluid gives rise to increased scattered X-ray intensity in the low q region (Figure 3). This scattering data can be used as a convenient means to assess changes in nanoparticle size arising from particle growth upon encapsulation in the complex fluid matrix. That is, standard Guinier analysis can be applied to SAXS data in the region where the momentum transfer, *q*, is small compared with the particle dimensions, $qR_g \leq 1$, where R_g is the radius of gyration.[36] For the samples containing the hydrophilic silver nanoparticles, low *q* corresponds to the region below the appearance of the first-order Bragg peak. In this region, a plot of $\ln[I(q)]$ versus q^2 will yield a line of slope R_g. By

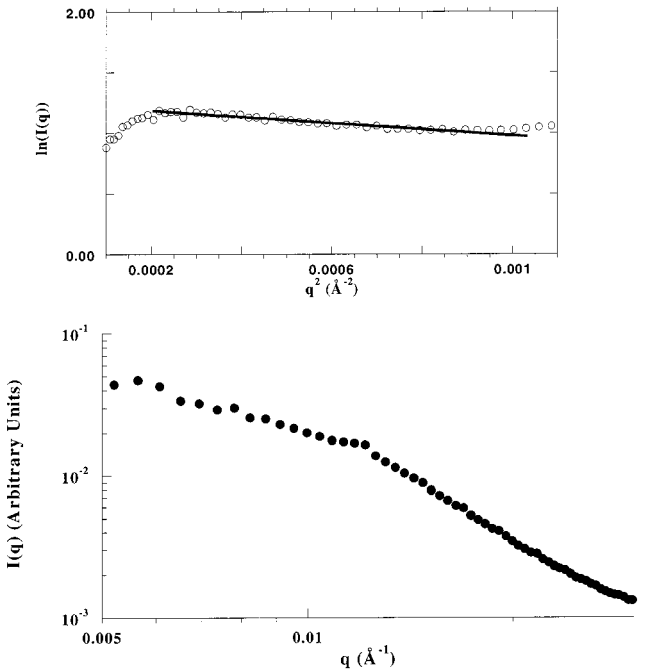

Figure 4. Log-log plot of the low q synchrotron small-angle X-ray scattering pattern collected on a PEG5000 grafted lipid complex fluid composition at 23 °C. Inset is Guinier plot of low q scattering data (°). The solid line represents a linear least-squares fit to the experimental data.

assuming spherical particles, the average radius of the particles, R, can be determined from $R_g = \sqrt{3/5}$ R. This simple analysis can be conducted on the samples in which alterations in the absorption spectra were observed (e.g., PEG5000 grafted lipid composition doped with bare silver colloid) in order to determine if these changes arise from particle aggregation or size growth upon encapsulation into the lamellar gel structure. An example of such an analysis is presented in Figure 4, which depicts the low q scattering profile collected for bare Ag nanoparticles intercalated into a complex fluid prepared with lipid appended PEG 5000 (113 repeat units). The attenuation (turn over) of the scattered X-ray intensity observed at very low q ($q^2 < 0.0002$) is characteristic of repulsive interparticle interactions.[37] Guinier analysis (inset of Figure 4) of these data yields a R_g of 27.7± 0.8 Å, corresponding to an average particle diameter of 71.5 ± 1.9 Å. This particle size is in good agreement with the results of TEM measurements performed on the colloidal solutions prior to incorporation in the gel, which indicated a particle size distribution between 60 and 83 Å. These results suggest that it is unlikely that aggregation/particle growth of the colloidal Ag occurs upon its incorporation into the complex fluid matrix. This result, in conjunction with the observed changes in the surface plasmon resonances (vida supra), indicates that the underivatized silver nanoparticles, although closely packed within the aqueous domains of the Lαg phase, remain as individual particles.

In summary, the results presented here demonstrate that polymer-grafted, lipid-based complex fluids can be successfully employed as a scaffolding for the formation of nanoparticle arrays. The use of complex fluids allows for the facile, single-step construction of nanoparticle-based materials by simple introduction of discrete nanoparticles, either as a hydrosol (for introduction of the hydrophilic colloidal nanoparticles) or as the isolated, dry powder (for hydrophobic nanoparticles), into the complex fluid at the time of its preparation. Our results also demonstrate that the nanoparticles can be directed into any of the three physicochemically distinct regions of the host matrix by controlling their size and surface characteristics and that the noncovalent supramolecular architecture of the complex fluid remains largely intact upon nanoparticle incorporation. In addition, simple modification of the complex fluid composition, by increasing the number of repeat units on the lipid appended PEG moieties, offers a means to modulate interactions of encapsulated nanoparticles and hence, their optical and electronic properties. A more detailed picture of the structural organization of the nanoparticles within the various segregated domains of the liquid crystal should be achievable by anomolous X-ray scattering measurements, which will be described in a future report.

The use of complex fluids offers considerable potential as an economical wet chemical approach to the production of nanostructured materials. Most importantly, the complex fluids can be used as a scaffolding for the creation of nanoparticle heterostructured composites such as semiconductor-metal or magnet-semiconductor. Exploration of such materials will be the focus of future work, as will exploiting the structural phase transitions of the complex fluids (i.e., temperature induced transformations from hexagonal to lamellar phase) as a means to tune encapsulated nanocrystal organization and hence, physicochemical properties.

Acknowledgment. This work was performed under the auspices of the Office of Basic Energy Sciences, Division of Materials Science, U. S. Department of Energy, under Contract No. W-31-109-ENG-38. The authors would like to thank the BESSRC staff (APS-ANL) for experimental assistance, Dr. D. Tiede for use of his spectrophotometer for these studies and most importantly, Dr. J. Nedelijkovic for many helpful discussions regarding metal nanoparticles.

References

(1) Heath, J. R.; Knobler, C. M.; Leff, D. V. *J. Phys. Chem. B* **1997**, *101*, 189−197.
(2) Murray, C. B.; Kagan; Bawendi, M. G. *Science* **1995**, *270*, 1335−1338.
(3) Korgel, B. A.; Fullam, S.; Connolly, S.; Fitzmaurice, D. *J. Phys. Chem. B* **1998**, *102*, 8379−8388.
(4) Martin, J. E.; Wilcoxon, J. P.; Odinek, J.; Provencio, P. *J. Phys. Chem. B* **2000**, *104*, 9475−9486.
(5) Li, H. X.; Lin, M. Z.; Hou, J. G. *J. Crystal Growth* **2000**, *212*, 222−226.
(6) Manoz, R.; Frydman, E.; Cohen, S. R.; Sagiv, J. *Adv. Mater.* **2000**, *12*, 725−727.
(7) Fendler, J. H.; Meldrum, F. *Adv. Mater.* **1995**, *7*, 607−631.
(8) Loweth, C. J.; Caldwell, W. B.; Peng, X.; Alivisatos, A. P.; Schultz, P. G. *Angew. Chem., Int. Ed. Engl.* **1999**, *38*, 1808−1812.
(9) Storhoff, J. J.; Lazarides, A. A.; Mucic, R. C.; Mirkin, C. A.; Letsinger, R. L.; Schatz, G. C. *J. Am. Chem. Soc.* **2000**, *122*, 4640−4650.
(10) Mann, S.; Shenton, W.; Li, M.; Connolly, S.; Fitzmaurice, D. *Adv. Mater.* **2000**, *12*, 147−150.
(11) Connolly, S.; Rao, S. N.; Fitzmaurice, D. *J. Phys. Chem. B* **2000**, *104*, 4765−4776.
(12) Sarathy, K. V.; Thomas, P. J.; Kulkarni, G. U.; Rao, C. N. R. *J. Phys. Chem. B* **1999**, *103*, 399.

(13) Musick, M. D.; Keating, C. D.; Lyon, A.; Botsko, S. L.; Pena, D. J.; Holliway, D.; McEvoy, T. M.; Richardson, J. N.; Natan, M. J. *Chem. Mater.* **2000**, *12*, 2869−2881.
(14) Auer, F.; Scotti, M.; Ulman, A.; Jordan, R.; Sellergren, B.; Garno, J.; Liu, G. Y. *Langmuir* **2000**, *16*, 7554−7557.
(15) Aliev, F.; Correa-Duarte, M.; Mamedov, A.; Ostrander, J. W.; Geirsig, M.; Liz-Marzan, L.; Kotov, N. *Adv. Mater.* **1999**, *11*, 1006−1010.
(16) Svergun, D. I.; Shtykova, E.; Kozin, M. B.; Volkov, V. V.; Dembo, A. T.; Shtykova, E. V.; Bronstein, L. M.; Platonova, O. A.; Yakunin, A. N.; Valetsky, P. M.; Khokhlov, A. R. *J. Phys. Chem. B* **2000**, *104*, 5242−5250.
(17) Wang, W.; Efrima, S.; Regev, O. *J. Phys. Chem. B* **1999**, *103*, 5613−5621.
(18) Firestone, M. A.; Thiyagarajan, P.; Tiede, D. M. *Langmuir* **1998**, *14*, 4688−4698.
(19) Firestone, M. A.; Tiede, D. M.; Seifert, D. M. *J. Phys. Chem. B* **2000**, *104*, 2433−2437.
(20) Silver hydrosols were prepared by sodium borohydride (5 mg) reduction of 1×10^{-4} M $AgNO_3$ aqueous solution (50 mL) under an inert atmosphere to yield a yellow solution containing underivatized Ag nanoparticles. Hydrophilic, surfactant-stabilized silver sols were prepared by inclusion of 0.01% (w/v) of lithium dodecyl sulfate to the 1×10^{-4} M aqeuous solution of $AgNO_3$ followed by reduction with $NaBH_4$.
(21) Samples for transmission electron microscopy measurements were prepared by placing 1−2 drops of colloidal nanoparticles onto holey carbon films supported on copper grids. The specimens were allowed to dry for at least 12 h prior to imaging. Samples were examined using a JEOL 100CXII Transmission Electron Microscope operating at 100 kV.
(22) Mafune, F.; Kohno, J.; Takeda, Y.; Kondow, T.; Sawabe, H. *J. Phys. Chem. B* **2000**, *104*, 8333−8337.
(23) Silver organosols were prepared by transfer of 0.003 M Ag(I) from aqueous solution (25 mL) into equal parts toluene using the phase transfer agent tetraoctylammonium bromide($[CH_3(CH_2)_{17}]_4NBr$). Extraction of the organic phase and addition of 0.2 mL of neat 1-dodecanethiol was followed by reduction by slow addition (over a 1 h time frame) of an aqueous 0.4 M $NaBH_4$ solution with vigorous stirring. The solution immediately turned yellow but upon further addition of $NaBH_4$, became red, and finally, orange-brown. The reaction was allowed to proceed for 2 h following addition of the reducing agent. The organic phase was then removed under vacuum to isolate the dry dodecanthiolated silver nanoparticles. The isolated particles were purified (to remove unreacted phase transfer reagent and dodecanthiol) by diluting with ethanol (120 mL) followed by suction filtration, yielding a waxy orange-brown solid.
(24) Brust, M.; Walker, M.; Bethell, D.; Schiffrin, D. J.; Whyman, R. *J. Chem. Soc. Chem. Commun.* **1994**, 801−802.
(25) Linnert, T.; Mulvaney, P.; Henglein, A. *J. Phys. Chem.* **1993**, *97*, 679−682.
(26) Henglein, A. *Ber. Bunsen-Ges. Phys. Chem.* **1995**, *99*, 903−913.
(27) PEG2000-based compositions of the lamellar gel phase (Lαg) of the complex fluid consisted of 0.796 ± 0.001 weight fraction, ϕ_w, of water, $\phi_s = 0.030 \pm 0.030$ lauryldimethylamino *N*-oxide (Calbiochem−Novabiochem Corp., La Jolla, CA), $\phi_L = 0.174 \pm 0.005$ (DMPC and DMPE, Avanti Polar Lipids, Alabasater, AL), with PEG2000 (MW = 2000; $n = 45$ monomer units) grafted phospholipid to total phospholipid content of 8.0 mol %. PEG5000-based compositions of were composed by 0.782 ± 0.002 weight fraction, ϕ_w, of water, $\phi_s = 0.029 \pm 0.001$ lauryl dimethylamino *N*-oxide, $\phi_L = 0.184 \pm 0.004$ (DMPC and DMPE), with PEG5000 (MW = 5000; $n =$ 113 monomer units) grafted phospholipid to total phospholipid content of 6.5 mol %. Hydration of the solid components was carried out with either water (undoped and dodecanthiol-derivatized Ag particle phases) or Ag hydrosols (bare Ag or LDS-stabilized Ag nanoparticles) by repeated cycles of warming to 35 °C, vortexing, and cooling on an ice bath until uniform transparent elastic solid/gels were formed at room temperature.
(28) Creighton, J. A.; Eadon, D. G. *J. Chem. Soc., Faraday Trans.* **1991**, *87*, 3881−3891.
(29) Vuvkovic, V. V.; Nedelijkovic, J. M. *Langmuir* **1993**, *9*, 980−983.
(30) Kang, S. Y.; Kim, K. *Langmuir* **1998**, *14*, 226−230.
(31) Ung, T.; Liz-Marzan, L. M.; Mulvaney, P. *Langmuir* **1998**, *14*, 3740−3748.
(32) Henglein, A.; Meisel, D. *J. Phys. Chem. B* **1998**, *102*, 8364−8366.
(33) Farbman, I.; Efrima, S. *J. Phys. Chem.* **1992**, *96*, 8469−873.
(34) Synchrotron small-angle X-ray scattering measurements were performed on the BESSRC undulator beamline (12ID-C) of the Advanced Photon Source (APS) at Argonne National Laboratory (ANL). The scattering profiles were recorded with a mosaic detector consisting of 9 CCD chips with an imaging area of 15 × 15 cm, and 1536 × 1536 pixel resolution. The sample-to-detector distance was set such that the detecting range for momentum transfers of $0.008 < q < 0.8$ Å^{-1} for high q and $0.0051 < q < 0.17$ Å^{-1} for low q studies, respectively. The area detector images were corrected for background scattering of water by subtracting from the recorded images an area detector image of a water sample obtained with the same total exposure time as for the complex fluid samples (1 s). The collected scattering data were calibrated on the basis of the known positions of silver behenate powder Bragg reflections. All samples were measured within 1 week of preparation.
(35) Guinier, A. *X-ray Diffraction in Crystals, Imperfect Crystals, and Amorphous Bodies*; Dover Publications, Inc.: New York, 1994.
(36) Guinier, A.; Fournet, G. *Small Angle Scattering of X-rays*; John Wiley & Sons, Inc.: New York, 1955.
(37) Rajh, T.; Thurnauer, M. C.; Thiyagarajn, P. *J. Phys. Chem. B* **1999**, *103*, 2172−2177.

NL0155025